

Preparation and Characterization of Lignin Graft Copolymer as a Filtrate Loss Control Agent for the Hydrocarbon Drilling Industry

M. N. Mohamad Ibrahim,* Say Liang Lim, M. R. Ahmed-Haras, and F. S. Fayyadh

Lignin graft copolymer (LGC) was prepared using an addition polymerization technique that involved grafting a 2-acrylamido-2-methylpropane sulfonic acid (AMPS) monomer onto soda lignin (SL). The optimal polymerization conditions were found to be as follows: soda lignin, 2.0 g; initiator, 3% (w/w) potassium persulphate of SL; mass ratio of AMPS to SL, 1:2; reaction time, 7 h; and reaction temperature, 60 °C. The LGC was characterized using a Fourier transform infrared (FTIR) spectroscopy, a thermogravimetric analyzer (TGA), and gel permeation chromatography (GPC). The filtrate loss controlling ability of the LGC was evaluated using the American Petroleum Institute Recommended Practice 13-B 1 standard procedures. The results showed that the LGC has remarkable rheological and filtration controlling properties at both room temperature and high aging temperatures (190 °C).

Keywords: Oil palm empty fruit bunch fibers; Graft copolymer; Soda lignin; AMPS; Addition polymerization; Filtrate loss

Contact information: Lignocellulosic Research Group, School of Chemical Sciences, Universiti Sains Malaysia, 11800 Minden, Pulau Pinang, Malaysia; *Corresponding author: mnm@usm.my

INTRODUCTION

Today, rotary drilling is the system most widely used in drilling rigs, especially for oil and gas exploration. This system incorporates several important components, *i.e.*, drilling equipment, mud pits, Kelly, swivel, rotary table, drilling pipes, bits, and drilling fluids (Bourgoyne *et al.* 1991). Over the course of drilling an oil well, many obstacles, such as hole instability, loss of circulation, fluid loss, and pipe sticking, are encountered because of the hostile conditions of geological formations. Because most of the drilling issues are interrelated with drilling fluid, the quality of the drilling fluid is a critical factor for ensuring the success of the drilling operation (Petri and Queiroz Neto 2010).

Specifically, fluid loss occurs when the liquid phase of the drilling fluid flows into the permeable formation because the borehole pressure is higher than the formation pressure. As a consequence of fluid loss, other drilling problems such as excessive torque and drag, differential pressure sticking, borehole instability, and formation damage, may flare up during the drilling operation (Jiao and Sharma 1994). Typically, a filtration control agent is added to the drilling fluid to reduce the water loss and the filter cake thickness of the drilling fluid. However, most filtration control agents have limitations such as degradation at high temperatures (above 150 °C) and low tolerance to salinity. Therefore, there is a need for an alternative filtration loss controlling agent to overcome these problems.

In past few years, attention has been paid to the development of polymeric material from natural lignocellulosic fibers from pine needles, *Hibiscus sabdariffa*,

Grewia optiva, jute, flax and oil palm fibers due to increasing environmental awareness and (Thakur *et al.* 2010). Every year, approximately 90 million tons of renewable oil palm biomass, including trunks, fronds, shells, palm press fibers, and empty fruit bunches, are generated by the Malaysian oil palm industry (MPOB 2013). Oil palm empty fruit bunch fibers (OPEFB) exhibit high potential for use in the paper mill industry, especially in Malaysia (Wan Daud and Law 2011). In the pulping process, large amounts of effluent (black liquor) are produced and need a proper treatment before they can be discharged. The black liquor is considered toxic to the environment due to its high alkalinity and dissolved solids. Many valuable dissolved solids such as cellulose, hemicelluloses, lignin, and degradation products can be recovered through the treatment of black liquor (Wallberg *et al.* 2006). It is undeniable that lignin isolated from OPEFB black liquor is highly promising and has great potential for use as a raw material in industrial applications such as epoxy, biodispersants, foams, and phenolic powder resins (Lora and Glasser 2002), as it is abundant and low-cost.

Due to its significant thermal stability, lignin has the potential to be used as an additive for drilling fluid. According to results obtained in previous studies (Panesar *et al.* 2013; Wei *et al.* 2002), a novel lignin graft copolymer can be prepared by exploiting lignin recovered from OPEFB through an addition polymerization reaction. The aim of this study was to present a method for the preparation of a lignin graft copolymer, namely AMPS-g-SL, and to provide a preliminary evaluation of the AMPS-g-SL as a water-based filtrate loss control agent for water-based drilling fluid.

EXPERIMENTAL

Materials

Soda lignin (SL) was recovered from oil palm empty fruit bunch fibers through the pulping process (Sun and Tomkinson 2001). AMPS (2-acrylamido-2-methylpropanesulfonic acid) monomers with 99% purity were purchased from Merck (Merck, Germany), while the initiator, potassium persulphate ($K_2S_2O_8$), was obtained from Sigma (Sigma Aldrich, USA). The sodium hydroxide, sulfuric acid, calcium carbonate, and sodium chloride that were used in this study were of analytical grade and were purchased from Qrec (Qrec, New Zealand). The clay (bentonite) used in the drilling fluid properties tests was obtained from SCOMI Oil tools (M) Sdn. Bhd. All the chemicals were used as received.

Recovery and Purification of Soda Lignin

The pulping process was conducted in accordance with the modified methods of Sun and Tomkinson (2001). The OPEFB long fiber was weighted in the ratio of 1:10 (w/w) to sodium hydroxide aqueous solution (cooking liquor) and soaked in water for 2 days to remove non-fibrous materials. The cooking liquor was prepared by dissolving 250.0 g of sodium hydroxide into 7 L of distilled water. A laboratory-scale 10-L stainless steel rotary digester was used to pulp the OPEFB long fiber.

Then, the black liquor obtained from the pulping process was filtered. The SL was precipitated from the black liquor using 20% (v/v) sulfuric acid until the black liquor solution reached pH 2. The precipitate was filtered and washed with distilled water. The SL was collected and dried in a vacuum oven at 55 °C for 48 h. Using a Soxhlet apparatus, the SL was purified with n-pentane for 6 h to remove the waxes and lipids.

Next, the precipitate was filtered and washed with distilled water. Finally, the purified SL was dried in an oven at 55 °C for another 48 h to remove any excess moisture.

Preparation of AMPS-g-SL

In order to obtain the optimized conditions of graft copolymerization, the reaction was carried out in a three-necked round-bottomed flask attached to a reflux condenser and equipped with a nitrogen inlet and thermometer. Figure 1 shows the suggested reaction mechanism for grafting the 2-acrylamido-2-methylpropane sulfonic acid (AMPS) monomers onto the SL. Appropriate amount of SL, AMPS, and potassium persulphate were dissolved at a 1% concentration into a 100-mL sodium hydroxide aqueous solution. Then, the mixture was flushed with nitrogen gas for 10 min. The grafting reaction was conducted at different temperatures for a period of time with vigorous stirring. After the reaction was completed, the solution was precipitated using 10 mL of 20% (v/v) sulfuric acid. The solvent was isolated in a centrifuge at a speed of 3000 rpm. To remove the unreacted monomers, the product was washed with distilled water and dried at 55 °C until a constant weight was obtained. The percent yield of AMPS-g-SL and percentage grafting ratio in each batch of reaction were determined using Eqs. 1 and 2, respectively.

$$\% Y = \frac{W_t}{W_A + W_S} \times 100 \% \quad (1)$$

$$\% GR = \frac{W_t - W_S + W_U}{W_S - W_U} \times 100 \% \quad (2)$$

where W_t is the total weight of AMPS-g-SL, W_S is the total weight of SL, W_A is the weight of the AMPS monomer, and W_U is the weight of the SL remaining in the supernatant (Fang *et al.* 2009).

Characterization of AMPS-g-SL

A Perkin Elmer 2000 FT-IR spectrometer was used to detect the functional groups of AMPS-g-SL and SL. Both samples were analyzed by means of a potassium bromide (KBr) pellet technique and scanned in the range of 4000 to 400 cm^{-1} at a resolution of 4%. The thermal degradation behaviors of AMPS-g-SL and SL were studied using a thermogravimetric analyzer (Mettler Toledo, model TGA/SDTA 851). Each of the samples was heated from 30 to 900 °C at a heating rate of 20 °C per min in a nitrogen atmosphere at a flow rate of 30 mL per min.

Molecular weight distribution of soda lignin and LGC were determined using gel permeation chromatography. Tetrahydrofuran (THF) was used as a mobile phase with a flow rate of 1.0 mLmin^{-1} using Water 1525 Binary HPLC Pump. Three Water Stryragel Column and Water 2414 refractive index detector were used in this system. Before analyzing the sample, the column was calibrated using a narrow molecular weight monodisperse polystyrene standard ranging from 580 to 8,500,000 gmol^{-1} in the eluent. The soda lignin and LGC were dissolved in THF at a concentration of 10 mgmL^{-1} . Then, the samples were filtered using Whatmann 0.45 μm membrane filter and 20 μL of sample was injected into GPC system.

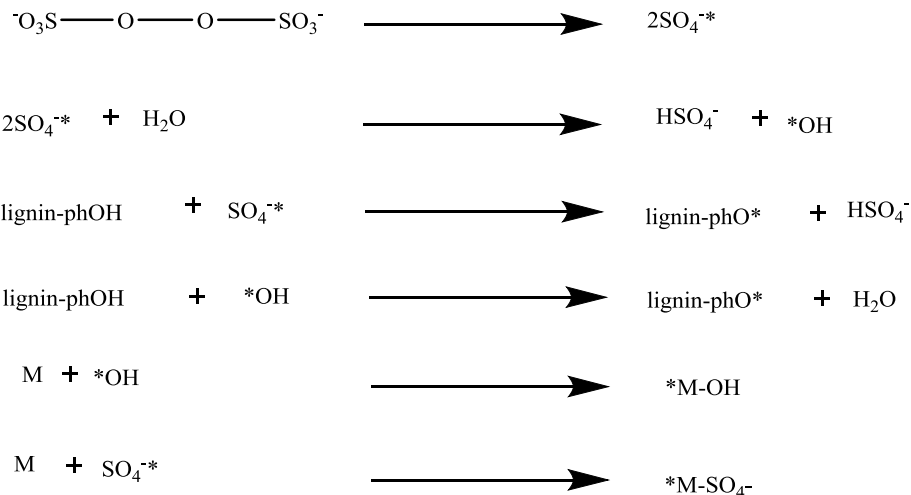
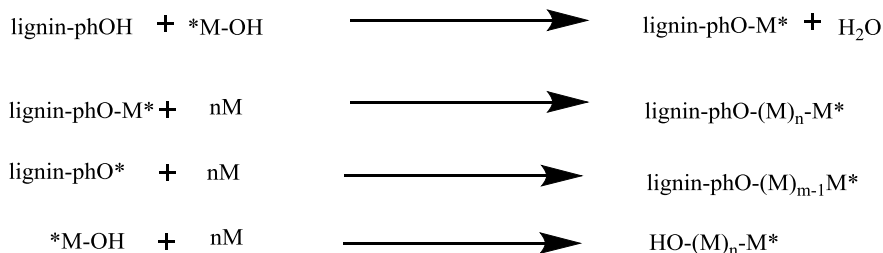
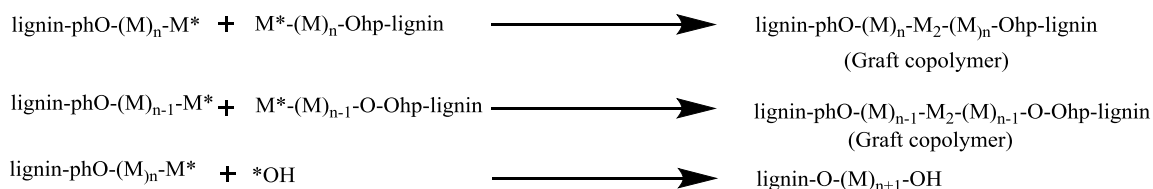
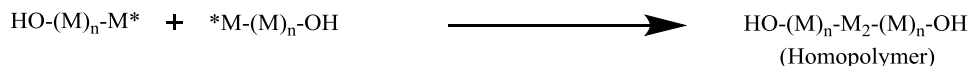
Initiation Reaction*Propagation Reaction**Termination Reaction**Disproportion of homopolymer*

Fig. 1. Suggested grafting reaction mechanism for grafting AMPS monomers onto SL; M* = monomer free radical, lignin-phO* = soda lignin free radical (Thakur *et al.* 2012)

Application of AMPS-g-SL

Each batch of a fresh water-based drilling mud was prepared by stirring 80.0 g of bentonite (clay) and 4.0 g of sodium carbonate in 1000 mL of distilled water before aging for 24 h (Zhang and Yin 1999; Wu *et al.* 2002). Salt water-based mud containing 80.0 g of bentonite, 20.0 g of sodium chloride, and 4.0 g of sodium carbonate was prepared by a similar procedure.

For the drilling fluid properties test, the rheological properties of the mud were analyzed using a Fann model 286 viscometer that was set to take measurements of mud viscosity at two rotating rates of 300 rpm (θ_{300}) and 600 rpm (θ_{600}). The apparent viscosity (μ_a), plastic viscosity (μ_p), and yield point (τ_y) were calculated using the following equations (American Petroleum Institute 2003):

$$\mu_a = \theta_{600} / 2 \quad (3)$$

$$\mu_p = \theta_{600} - \theta_{300} \quad (4)$$

$$\tau_y = 0.511(\theta_{300} - \mu_p) \quad (5)$$

where θ_{300} and θ_{600} are viscometer shear stress readings at 300 and 600 rpm, respectively. The standard deviation of each data was calculated. The API filtrate loss volume (FV_{API}) was determined using a Fann filter press model, series 300. The effects of aging temperature on the water-based mud rheological and filtration loss properties were evaluated using a Fann model rolling oven series 2500 and a 500-mL Fann stainless steel aging cell.

Two sets of water-based mud property tests, named Experiments I and II, were designed and evaluated according to the American Petroleum Institute Recommended Practice 13B-1 specifications (American Petroleum Institute 2003). In Experiment I, the effects of varying dosages of AMPS-g-SL in water-based drilling mud were studied at room temperature. The dosages that were introduced ranged from 0.3% to 1.5% (w/w) for fresh water-based mud and from 0.5% to 3.5% (w/w) for salt water-based mud. The effects of aging temperature on drilling mud containing AMPS-g-SL were evaluated in Experiment II. The mud samples were heated in a roller oven at 190 °C for 16 h.

RESULTS AND DISCUSSION

Characterization of SL and AMPS-g-SL

Fourier Transform Infrared (FT-IR) analysis

From the infrared spectrum of SL (Fig. 2), a broad band centered at 3436 cm^{-1} indicated the hydroxyl group (OH) of phenolic and aliphatic compounds (Mohamad Ibrahim *et al.* 2010). The peak at 2935 cm^{-1} was attributed to (C-H) stretching in the methyl groups. The stretch band at 1709 cm^{-1} was attributed to conjugated carbonyl (C=O) groups. Evidence of aromatic skeletal vibration of the aromatic rings (C=C) was found in the medium bands at 1606 cm^{-1} and 1511 cm^{-1} (Awal and Sain 2011). The peak at 1459 cm^{-1} was attributed to (C-H) deformations in the methyl, methylene, and methoxyl groups. Meanwhile, the peak at 1425 cm^{-1} was attributed to aromatic skeletal vibration and (C-H) in-plane deformations. The peaks at 1327 cm^{-1} and 1115 cm^{-1} corresponded to syringyl (S) ring breathing with (C-O) stretching and aromatic (C-H) in-plane deformations. The bands at 1217 cm^{-1} were attributed to syringyl and guaiacyl ring breathing with (C-O) stretching. The aromatic (C-H) in-plane deformation of guaiacyl-type lignin appeared in the band at 1034 cm^{-1} . The band at 914 cm^{-1} indicated that the aromatic ring (C-H) out of the plane. A band at 831 cm^{-1} was characteristic of a (C-H) out of plane in a p-hydroxyl phenylpropane unit.

In the spectrum of AMPS-g-SL, the broadband presence at 3425 cm^{-1} could be attributed to overlapping of the (OH) stretch of the phenolic content of SL with the NH group of AMPS. The band at 2937 cm^{-1} indicated the (C-H) stretch of the methyl group. The band at 1712 cm^{-1} indicated the (C=O) stretching of unconjugated ketone, carbonyl, and ester groups. The presence of a new band at 1661 cm^{-1} was assigned to the (C=O) stretching of the amide group and verified the grafting of the AMPS polymeric chain onto the SL backbone. The bands at 1607 cm^{-1} and 1514 cm^{-1} corresponded to (C-C) stretching in the aromatic ring of SL. The band at 1217 cm^{-1} indicated syringl and guaicyl rings with (C-O) stretching. The band at 1116 cm^{-1} was attributed to aromatic (C-H) in-plane deformation of syringl. A strong stretch at 1040 cm^{-1} may have been due to the (SO₃H) functional groups of AMPS. The strong stretching that occurred at 625 cm^{-1} was attributed to the (S-O) of the sulfonic acid group.

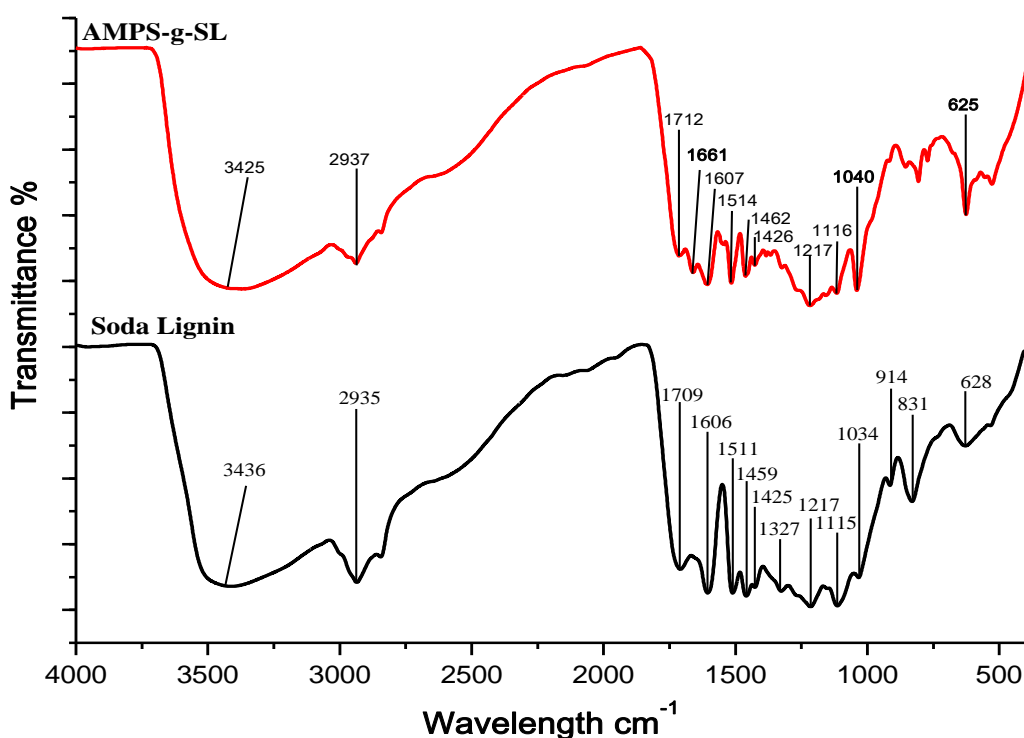


Fig. 2. FT-IR spectra of SL and AMPS-g-SL

Thermogravimetric analysis (TGA)

Figure 3 shows the first two thermal decomposition steps in the heating process of SL. The initial decomposition step of SL was recorded in the temperature range of 29.59 to 153.23 °C, with a 7.45% weight loss corresponding to water evaporation. The second decomposition step occurred in the range of 153.23 to 894.12 °C, with 55.94% weight loss attributed to fragmentation of the inter-unit linkages, which released carbon dioxide and monomeric phenols into the vapor (Elsaied and Nada 1993).

Figure 4 depicts the thermogram of AMPS-g-SL. The first decomposition step of the LGC occurred between the temperatures of 29.55 and 152.16 °C, with 10.70% weight lost attributed to the elimination of water. The second decomposition step covered the range of 152.16 to 254.22 °C, with 7.29% weight loss, and the third decomposition step witnessed temperatures in the range of 254.22 to 325.14 °C, with 8.92% weight loss.

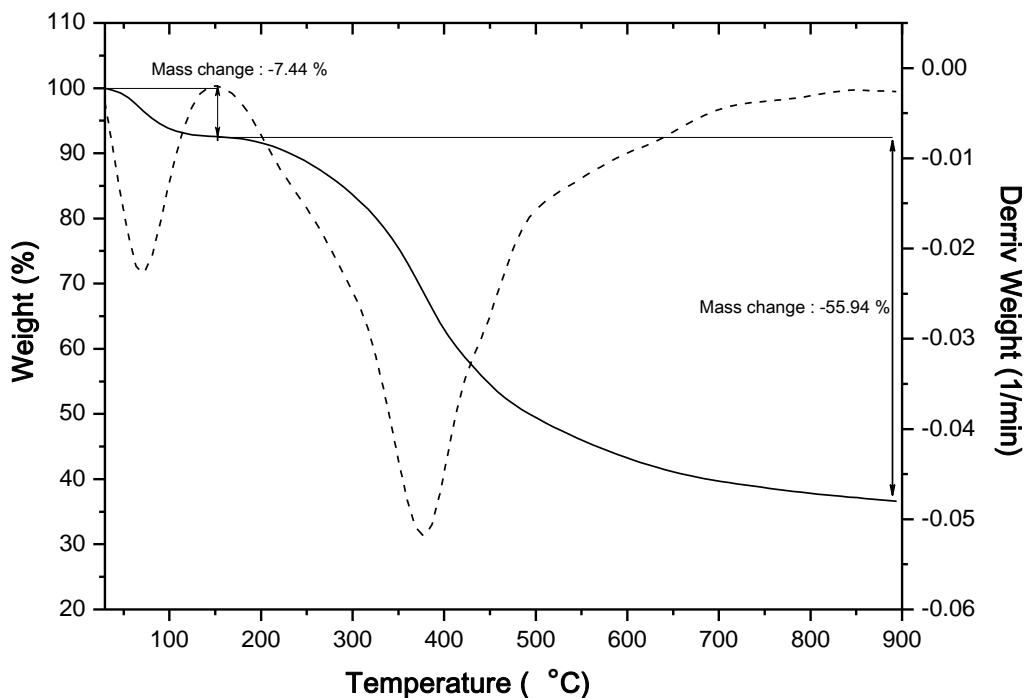


Fig. 3. TG thermogram of SL

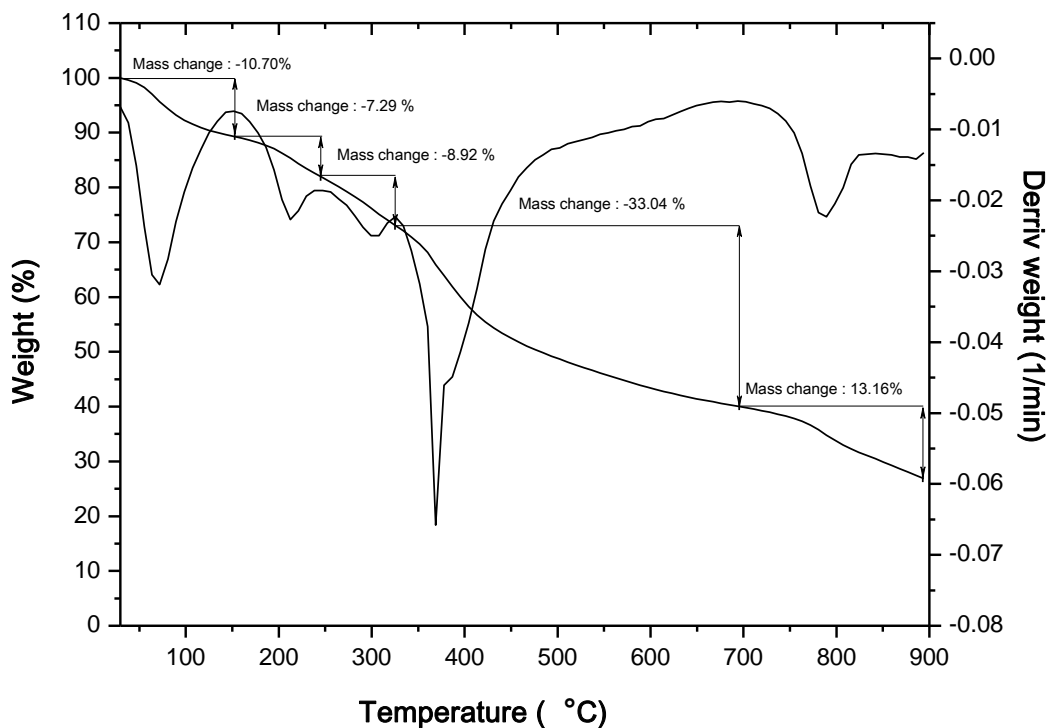


Fig. 4. TG thermogram of AMPS-g-SL

The second and third decomposition steps can be attributed to the instability of the sulphonic acid groups, which can be degraded to SO_2 and SO_3 (Qiao *et al.* 2005).

During the fourth decomposition step, temperatures were recorded in the range of 325.14 to 694.04 °C, with 33.04% weight loss that was attributed to the paralytic degradation of the lignin backbone structure, which released sulphur dioxide, carbon dioxide, and monomeric phenols into the vapor. The temperatures during the final decomposition step were recorded in the range of 694.04 to 892.91 °C, with 13.16% weight loss attributed to the release of carbon dioxide and the decomposition of the aromatic ring (Mansouri and Salvado 2006). The onset temperature of the maximum decomposition step of soda lignin was at 153.23 °C; in contrast, the onset temperature of the maximum decomposition step of AMPS-g-SL was at 325.14 °C. The difference in onset temperatures revealed that AMPS-g-SL has better thermal stability compared to soda lignin.

Gel Permeation Chromatography (GPC) analysis

The weight average (M_w), number average (M_n), and polydispersity of soda lignin and LGC are recorded in Table 1. The results indicated that M_w and M_n of LGC were greater compared to soda lignin. This is attributed to the polymeric chains of polyAMPS that was grafted onto the soda lignin backbone. In addition, high molecular weight also enhance the thermal property of the LGC.

Table 1. Gel Permeation Chromatography Data for Soda Lignin and LGC

| Sample | M_n (g/mol) | M_w (g/mol) | M_w/M_n (Polydispersity) |
|-------------|------------------|------------------|-------------------------------|
| Soda lignin | 909 | 1714 | 1.88 |
| LGC | 1315448 | 2665508 | 2.02 |

Optimization of Grafting Conditions

The graft co-polymerization reaction was conducted in numerous batches with the aim of discovering the optimum conditions for the reaction. The effects of the dosages of potassium persulphate and AMPS, reaction temperature, and time were studied such that the optimum reaction conditions could be estimated.

Effect of initiator dosage

To study the effect of initiator dosage on the percentage of yield and grafting ratio, the initiator dosage was varied from 1 to 5% of SL weight. The results, which are presented in Fig. 5, indicated that the percentage of yield and grafting ratio of the copolymer increased from 1 to 3% of the mass of SL. This could have been due to the increase in the rate of grafting at low initiator concentrations. Beyond this initiator dosage, the yield and grafting ratio decreased gradually. This may be attributable to the decrease in the rate of polymerization at higher initiator dosages and the increase in the rate of termination, particularly via bimolecular collisions between the two chain radicals species (Lokhande and Gotmare 1999). The percent yield and grafting ratio reached their maximum at the ideal initiator dosage of 3% of the mass of SL.

In the graft copolymerization reaction, potassium persulphate acts as an initiator, providing free radicals that create microradicals on the backbone of SL to which the AMPS or polyAMPS chains can be grafted (Abu Bakar *et al.* 2008). This initiator also initiates the polymerization of polyAMPS. Therefore, the concentration of initiator influenced and dictated the percent yield and grafting ratio in the reaction. The high dosage of initiator enhanced the possibility of graft copolymerization and increased the

yield and molecular weight; conversely, however, over high dosage of initiator will lower the polymerization degree of the polyAMPS that are able to graft onto the SL (Fang *et al.* 2009).

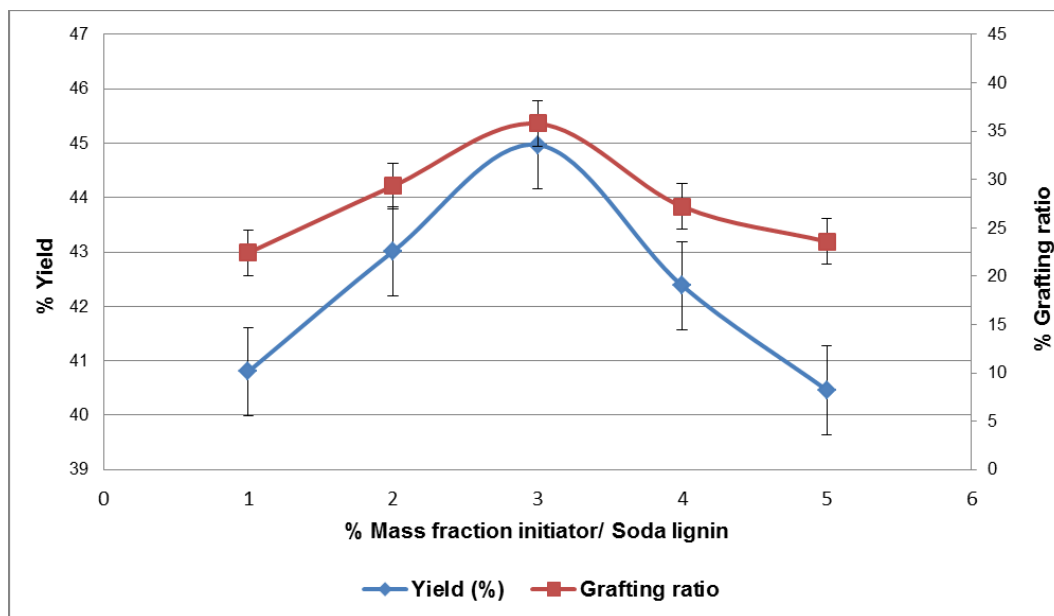


Fig. 5. Effect of initiator dosage on graft copolymer

Effect of AMPS dosage

The mass ratio of a 2-acrylamido-2-methyl propanesulfonic acid (AMPS) monomer is another parameter that influences the percentage of yield and grafting ratio. This parameter influences the graft copolymerization by adjoining the required number of AMPS units onto the SL backbone during the graft copolymerization reaction (Abu Bakar *et al.* 2008). To isolate the effects of the AMPS monomer, other reaction parameters, such as initiator dosage, reaction temperature, and time, were kept constant. As can be seen in Fig. 6, the results showed that the percent yield and grafting ratio initially increased rapidly. However, after the AMPS dosage exceeded 1.0 g, the percent yield and grafting ratio decreased gradually. This may have been due to the accumulation of the AMPS monomers in close proximity to the accessible hydroxyl groups on the SL, which would have sped up the graft copolymerization reaction and improved the percentage of grafting ratio. Nevertheless, when the dosage of AMPS was high, homopolymerization of AMPS started to occur, and polyAMPS was formed. PolyAMPS competed with SL and decreased the grafting ratio. The results indicated that the ideal dosage of AMPS was 1.0 g.

Effect of reaction time

The effects of reaction time on the graft copolymer were studied under predetermined conditions. The copolymerization was conducted for a variety of reaction times ranging from 2 to 7 h. Figure 7 presents the effect of reaction time on the graft copolymer. Between the reaction times of 2 and 6 h, the percent yield and the grafting ratio increased gradually. When the reaction time exceeded 6 h, the percent yield and grafting ratio became relatively constant.

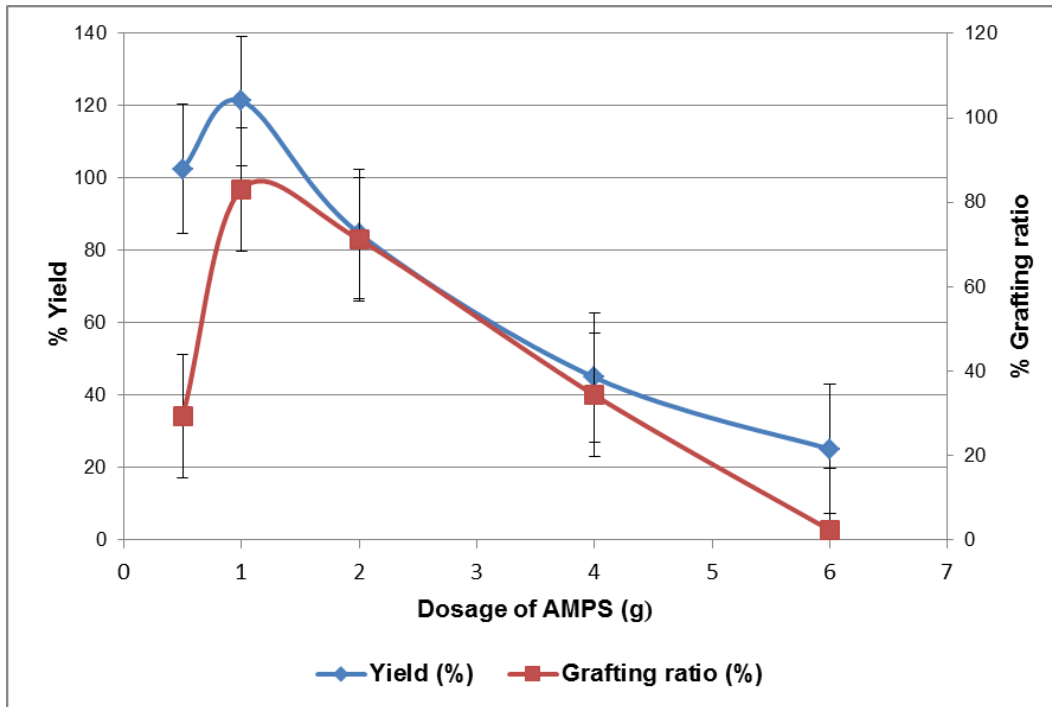


Fig. 6. Effect of AMPS dosage on graft copolymer

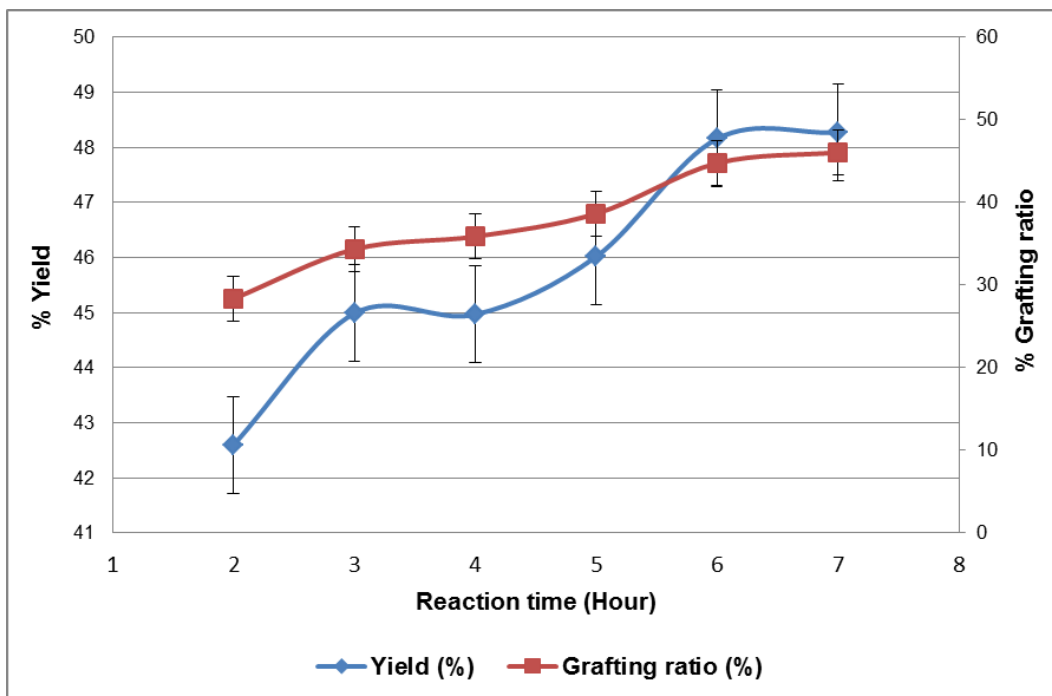


Fig. 7. Effect of reaction time on graft copolymer

The optimum reaction time was 7 h, with a percent yield of 48% and a grafting ratio of 46%. The initial growth in the grafting ratio was attributed to the increase in the quantity of active sites and the extension of the initiation and propagation with time (Ibrahim *et al.* 2005; Wang and Xu 2006). However, a retardation of diffusion occurred

after some of the polymers had formed on the SL surface. The relative deceleration of the percent yield and grafting ratio were attributed to the decline in the number of monomers and the initiator as time increased (Abu-Ilawi *et al.* 2004; Behari and Pandey 2006).

Effect of temperature

The graft copolymerization reactions were conducted at various reaction temperatures ranging from 30 to 70 °C. The results are depicted in Fig. 8. The percent yield and grafting ratio increased from 30 to 60 °C, but decreased thereafter. The increase in the percent yield and the grafting ratio before 60 °C could be attributed to the increase in the decomposition rate of the initiator and its contribution to the initiation of the grafting copolymerization (Naguib 2002). On the other hand, the higher temperature led to a decrease in the rate of grafting. When the temperature exceeded 60 °C, the percent yield and the grafting ratio declined due to the shorter half life of the initiator and caused increased of radical termination (Samaha *et al.* 2005).

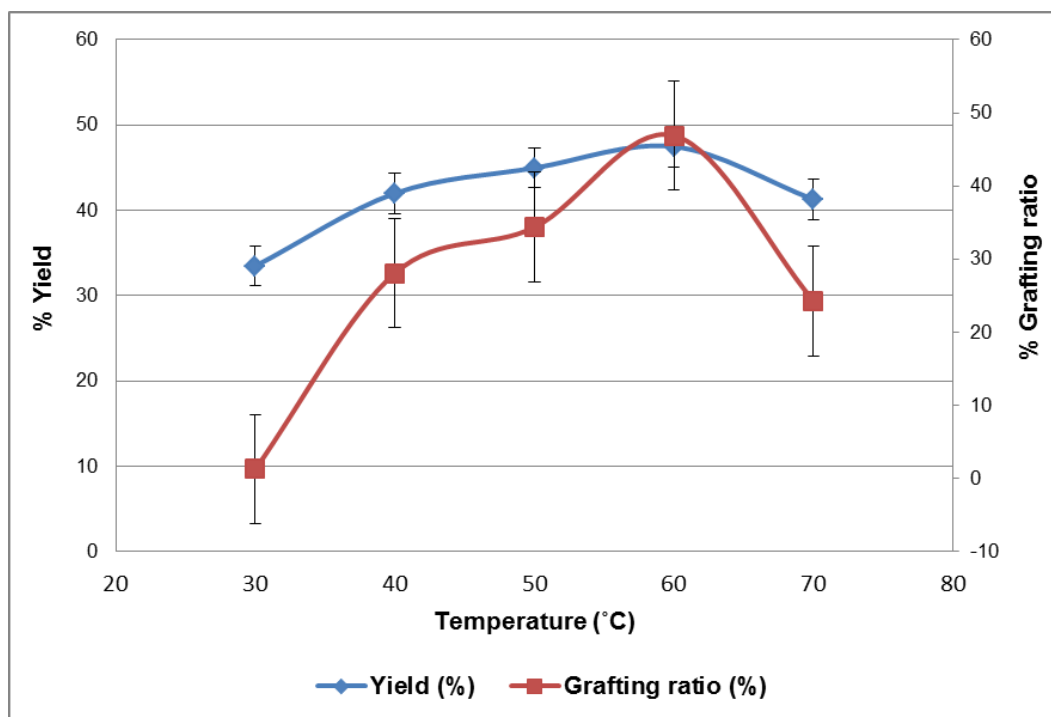


Fig. 8. Effect of reaction temperature on graft copolymer

Application of AMPS-g-SL

The effects of AMPS-g-SL dosage on the rheological properties of fresh water- and salt water-based drilling fluids are presented in Tables 2 and 3, respectively. The rheological data are presented so as to demonstrate the effects of the dosage additive on the drilling fluid rheology. With the addition of the graft copolymer into the corresponding freshwater-based mud, all the rheological parameters, including apparent viscosity (μ_a), plastic viscosity (μ_p), and yield point (τ_y), remained stable at room temperature and underwent no significant changes. In contrast, the apparent viscosity and plastic viscosity of the salt water-based drilling fluid increased slightly with the increase in the dosage of graft copolymer. However, the yield point was reduced with the increase

in the dosage of graft copolymer. It can be inferred that the presence of AMPS-g-SL does not affect the rheological properties of water-based mud significantly.

The effects of AMPS-g-SL dosage on the API filtrate volume of fresh water- and salt water-based drilling fluids before and after rolling are depicted in Figs. 9 and 10, respectively. The results clearly indicated that the API filtrate volume for both types of water-based drilling fluids was reduced gradually with the increase in the dosage of AMPS-g-SL. Due to the AMPS-g-SL absorbance of clay particles at the sites, a thicker hydrated shell was formed, thereby strengthening the clay structure and stabilizing the aqueous dispersion of clay particles (Guo and Peng 2012). As a result of the introduction of a 1.5% (w/w) additive into the fresh water-based mud, 50% of the API filtrate volume was reduced. The API filtrate volume of the salt water-based formulation mud also demonstrated a similar trend: a 76% drop in the filtrate loss volume was observed as a result of the addition of a 3.5% (w/w) dosage of graft copolymer to the salt water-based mud. The optimum dosages of AMPS-g-SL for the fresh and salt water-based muds were found to be 1.5% (w/w) and 3.5% (w/w), respectively.

Table 2. Rheological Properties of Fresh water-Based Mud under Different AMPS-g-SL Dosages (Before and After Thermal Aging Test)

| Additive dosage (%) | μ_a (mPa.s) | | μ_p (mPa.s) | | τ_y (Pa) | |
|---------------------|-----------------|------------|-----------------|------------|---------------|-----------|
| | Before | After | Before | After | Before | After |
| 0 ^a | 7.83±2.02 | 13.83±3.17 | 4.33±1.15 | 12.33±2.30 | 3.57±1.35 | 1.53±0.88 |
| 0.3 | 7.33±0.57 | 14.25±0.35 | 5.00±0.00 | 10.50±2.12 | 2.38±0.58 | 3.81±2.55 |
| 0.6 | 7.66±1.60 | 17.50±4.94 | 5.66±2.88 | 10.50±2.12 | 2.19±1.46 | 1.76±0.33 |
| 0.9 | 7.66±1.15 | 14.00±0.00 | 6.00±1.73 | 12.00±0.00 | 1.70±0.58 | 2.02±0.02 |
| 1.2 | 8.33±0.28 | 12.00±0.00 | 6.33±0.57 | 10.00±0.00 | 1.87±0.29 | 2.02±0.02 |
| 1.5 | 8.50±0.50 | 12.00±0.00 | 6.33±0.57 | 11.00±0.00 | 2.19±1.05 | 1.76±0.33 |

*All rheological data listed above were measured at 30 ± 0.5 °C. 0^a represents base mud

Table 3. Rheological Behavior for Salt water-Based Mud under Different AMPS-g-SL Dosages (Before and After Thermal Aging Test)

| Additive dosage (%) | μ_a (mPa.s) | | μ_p (mPa.s) | | τ_y (Pa) | |
|---------------------|-----------------|------------|-----------------|------------|---------------|-----------|
| | Before | After | Before | After | Before | After |
| 0 ^a | 10.0±1.00 | 12.00±0.00 | 3.33±0.57 | 10.00±0.00 | 6.79±1.55 | 2.02±0.02 |
| 0.5 | 9.50±0.00 | 14.00±0.00 | 5.33±1.52 | 8.00±0.00 | 3.23±1.18 | 6.08±0.07 |
| 1.0 | 9.50±0.00 | 12.33±0.28 | 7.00±0.00 | 9.00±1.73 | 2.53±0.02 | 2.53±0.02 |
| 1.5 | 8.91±0.72 | 9.50±0.50 | 7.16±0.28 | 9.00±0.00 | 1.76±0.45 | 0.50±0.00 |
| 2.0 | 12.00±0.00 | 8.33±1.15 | 10.00±0.00 | 8.00±0.00 | 2.02±0.02 | 1.01±0.01 |
| 2.5 | 13.58±2.40 | 14.66±2.46 | 10.16±3.88 | 12.00±0.00 | 3.46±1.97 | 1.52±0.01 |
| 3.0 | 11.00±0.00 | 17.33±0.28 | 7.00±0.00 | 15.00±0.00 | 4.05±0.04 | 2.53±0.02 |
| 3.5 | 11.00±0.00 | 18.00±0.00 | 7.00±0.00 | 15.33±0.57 | 4.05±0.04 | 2.70±0.61 |

*All rheological data listed above were measured at 30 ± 0.5 °C. 0^a represents base mud

The effects of thermal aging temperature were studied to address the problem of the slow degradation of drilling fluid constituents when left static in high-temperature environments for long hours during drilling operations (Peng *et al.* 2010). This factor commonly results in deterioration of the rheological and filtrate loss properties of the

drilling fluid (Lu *et al.* 2012). The rheological properties, including apparent viscosity and plastic viscosity, of fresh and salt water-based mud treated with AMPS-g-SL increased after rolling. In contrast, before rolling, the yield point managed to hold steady and exhibited minor differences in comparison to the rheological parameters. This suggested that fresh- and salt water-based muds formulated with AMPS-g-SL are stable at elevated temperatures due to the high molecular weight of the chains and the complex structure of AMPS-g-SL.

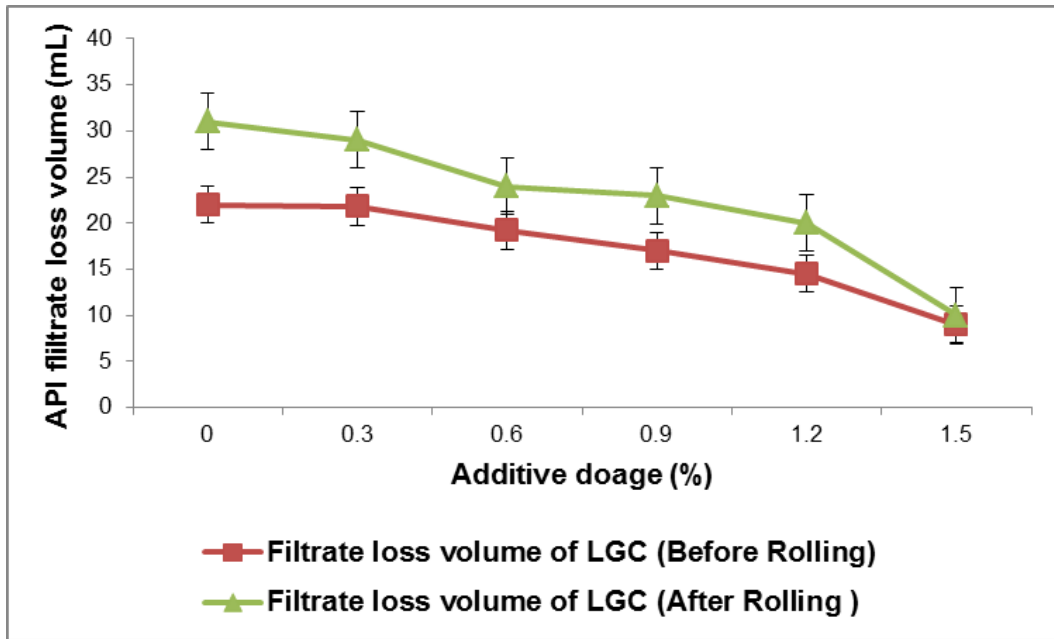


Fig. 9. Effect of AMPS-g-SL dosage on the filtrate loss volume of fresh water-based mud

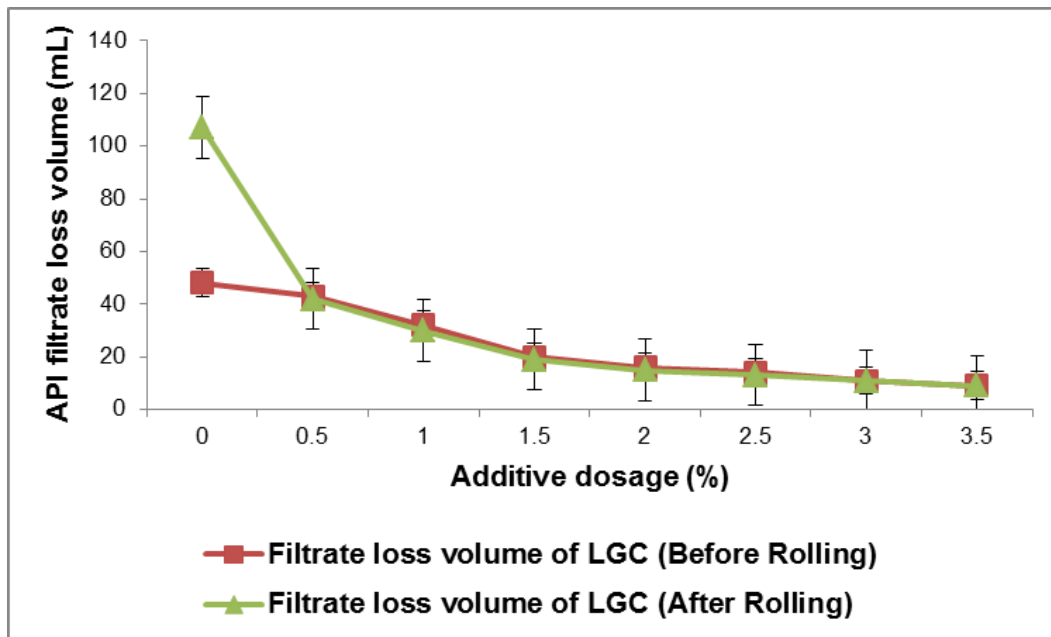


Fig. 10. Effect of AMPS-g-SL dosage on the filtrate loss volume of salt water-based mud

The API filtrate loss volume of fresh and salt water-based mud increased after rolling in comparison to before rolling, meaning that the elevated temperature (190 °C) was able to increase the permeability of the filter cake and destroy part of the mud gel structure (Wu *et al.* 2001). If aged at the elevated temperature of 190 °C, some clay aggregation may occur. However, the sample residual clay network was preserved, and the API filtrate volume of the sample remained in the acceptable range. This was because the AMPS-g-SL, which is highly branched and contains abundant hydration functional groups (*e.g.*, carboxyl groups) and adsorption functional groups (*e.g.*, acrylamide groups), adsorbed onto the clay particle surfaces (Peng *et al.* 2010). Consequently, the AMPS-g-SL plugged the filter cake holes and reduced the coefficients of penetration and filtration. Hence, the API filtrate volume decreased when the dosage of AMPS-g-SL increased.

CONCLUSIONS

1. Soda lignin was recovered from OPEFB fibers using the acid precipitation method, and lignin graft copolymer was successfully prepared via the addition polymerization technique.
2. The optimum conditions for graft copolymerization were as follows: 2.0 g of AMPS monomers grafted on 2.0 g of SL using a 3% mass fraction of SL of potassium persulphate at a temperature of 60 °C and for 7 h of reaction time.
3. The AMPS-g-SL showed good rheological and fluid loss controlling properties in water-based drilling fluids at a high temperature (190 °C).
4. The AMPS-g-SL was resistant under the salt water-based drilling fluid condition.

ACKNOWLEDGMENTS

The authors are grateful for the financial support from the Universiti Sains Malaysia under a research grant (304/PKIMIA/6312047).

REFERENCES CITED

- Abu Bakar, A., Nik Mat, N. S., and Kamaruddin Isnin, M. (2008). "Optimized conditions for the grafting reaction of poly(methyl methacrylate) onto oil palm empty fruit bunch fibers," *Journal of Applied Polymer Science* 110(2), 847-855.
- American Petroleum Institute. (2003). "Recommended practice standard procedure for laboratory testing drilling fluids," API Recommended Practice 13-1, 2nd edition, American Petroleum Institute, Washington D. C.
- Awal, A and Sain, M. (2011). "Spectroscopic studies and evaluation of thermorheological properties of softwood and hardwood lignin," *Journal of Applied Polymer Science* 122(2), 965-963.

- Behari, K., and Pandey, P. K. (2006). "Graft copolymerization of 2-acrylamido-2-methyl-1-propanesulfonic acid onto carboxymethylcellulose (sodium salt) by $\text{H}_2\text{O}_2/\text{Fe}^{2+}$ redox pair," *Journal of Applied Polymer Science* 100(6), 4819-4820.
- Bourgoyne Jr., A. T., Millheim, K. K., Chenever, M. E., and Young, F. S. (1991). *Applied Drilling Engineering*, Society of Petroleum Engineers Textbook Series, Texas.
- Elsaied, H., and Nada, A. (1993). "The thermal behaviour of lignins from wasted black pulping liquors," *Polymer Degradation and Stability* 40(3), 417-421.
- Fang, R., Cheng, X. S., Fu, J., and Zheng, Z. B. (2009). "Research on the graft copolymerization of EH-lignin with acrylamide," *Natural Science* 1(1), 17-22.
- Guo, W. Y., and Peng, B. (2012). "Synthesis and characterization of starch-graft-polyacrylamide copolymers and their application as filtration control agents in drilling fluid," *Journal of Vinyl & Additive Technology* 18(4), 261-266.
- Ibrahim, N. A., Abu-Illawi, F., Abdul Rahman, M. Z., Ahmad, M. B., Mohamd Dahlan, K. Z., and Wan Yunus, W. M. Z. (2005). "Graft copolymerization of acrylamide onto oil palm empty fruit bunch (OPEFB) fiber," *Journal of Polymer Research* 12(3), 173-179.
- Jiao, D., and Sharma, M. (1994). "Mechanism of cake buildup in crossflow filtration of colloidal suspensions," *Journal of Colloid and Interface Science* 162(2), 454-462.
- Lokhande, H. L., and Gotmare, V. D. (1999). "Utilization of textile loomwaste as a highly absorbent polymer through graft co-polymerization," *Bioresource Technology* 68(3), 283-286.
- Lora, J. H., and Glasser, W. G. (2002). "Recent industrial application of lignin: A sustainable alternative to non-renewable materials," *Journal of Polymers and Environment* 10(1-2), 39-48.
- Lu, H. S., Li, G. C., Dai, S. S., Zhang, T. L., Quan, H. P., and Huang, Z. Y. (2011). "Synthesis and properties of aminoacrylsulfonic acid-phenol-formaldehyde copolymer as drilling fluid loss reducer," *Journal of Macromolecular Science, Part A: Pure and Applied Chemistry* 49(1), 85-91.
- Mansouri, N. E., and Salvado, J. (2006). "Structural characterization of technical lignins for the production of adhesives: Application to lignosulfonate, kraft, soda-anthraquinone, organosolv and ethanol process lignins," *Industrial Crops and Products* 24(1), 8-16.
- Mohamad Ibrahim, M. N., Ahmed-Haras, M. R., Coswald, S. S., Aboul-Enein, H. Y., and Mohamed, A. A. (2010). "Preparation and characterization of a newly water soluble lignin graft copolymer from oil palm lignocellulosic waste," *Carbohydrate Polymer* 80(4), 1102-1110.
- Malaysia Palm Oil Board (MPOB). (2013). (<http://www.mpob.gov.my/>).
- Naguib, H. F. (2002). "Chemically induced graft copolymerization of itaconic acid onto sisal fibers," *Journal of Polymer Research* 9(3), 207-211.
- Panesar, S. S., Misra, M., and Mohanty, A. K. (2013). "Functionalization of lignin: Fundamental studies on a aqueous graft copolymerization with vinyl acetate," *Industrial Crops and Products* 46, 191-196.
- Peng, B., Peng, S. P., Long, B., Miao, Y. J., and Guo, W. Y. (2010). "Properties of high-temperature-Resistant drilling fluids incorporating acrylamide/(acrylic acid)/(2-acrylamido-2-methyl-1-propane sulfonic acid) terpolymer and aluminium citrate as filtration control agents," *Journal of Vinyl & Additive Technology* 16(1), 84-89.

- Petri, D. F. S., and Queiroz Neto, J. C. D. (2010). "Identification of lift-off mechanism failure for salt drill-in drilling fluid containing polymer filter cake through adsorption/desorption studies," *Journal of Petroleum Science and Engineering* 70(1), 89-98.
- Qiao, J., Hamaya, T., and Okada, T. (2005). "New highly proton-conducting membrane poly(vinylpyrrolidone)(PVP) modified poly(vinyl alcohol)/(2-acrylamido-2-methyl-1-propanesulfonic acid (PVA-PAMPS) for low temperature direct methanol fuel cells (DMFCs)," *Polymer* 46(24), 10809-10816.
- Samaha, S. H., Nasr, H. E., and Hebeish, A. (2005). "Synthesis and characterization of starch-poly(vinyl acetate) graft copolymers and their saponified form," *Journal of Polymer Research* 12(5), 343-353.
- Sun, R., and Tomkinson, J. (2001). "Fractional separation and physical-chemical analysis of lignins from the black liquor of oil palm trunk fibre pulping," *Separation and Purification Technology* 24(3), 529-539.
- Thakur, V. K., Singha, A. S., Kaur, I., Nagarajarao, R. P., and Yang, L. P. (2010). "Silane functionalization of *Saccharum cilliare* fibers: Thermal, morphological, and physicochemical study," *International Journal of Polymer Analysis and Characterization* 15(7), 397-414.
- Thakur, V. K., Singha, A. S., and Thakur, M. K. (2012). "In-air graft copolymerization of ethyl acrylate onto natural cellulosic polymers," *International Journal of Polymer Analysis and Characterization* 17(1), 48-60.
- Wallberg, O., Linde, M., and Jonsson, A. S. (2006). "Extraction of lignin and hemicelluloses from kraft black liquor," *Desalination* 199(1), 413-414.
- Wan Daud, W. R., and Law, K. N. (2011). "Oil palm fibers as paper making material: Potential and challenges," *BioResources* 6(1), 901-917.
- Wang, L., and Xu, Y. (2006). "Effect of dimethylaminoethyl methacrylate on the graft copolymerization of ethyl acrylate onto hydroxypropyl methylcellulose in aqueous medium," *Cellulose* 13(6), 713-724.
- Wei, X. M., Liu, X. L., Yu, Q. S., and Jiang, F. H. (2002). "Preparation of viscosity/fluid loss reducing additive MGAC-2 for water-base drilling fluids," *Oil Field Chemistry* 19(1), 15-18.
- Wu, Y. M., Sun, D. J., Zhang, B. Q., and Zhang, Ch. G. (2002). "Properties of high-temperature drilling fluids incorporating disodium itaconate/acrylamide/sodium 2-acrylamido-2-methylpropanesulfonate terpolymers as fluid loss reducers," *Journal of Applied Polymer Science* 83(14), 3068-3075.
- Zhang, L. M., and Yin, D. Y. (1999). "Novel modified lignosulfonate of drilling mud thinner without environmental concern," *Applied Polymer Science* 74(7), 1662-1668.

Article submitted: July 9, 2013; Peer review completed: October 20, 2013; Revised version received and accepted: January 23, 2014; Published: January 30, 2014.